

Chapter 5

Numerical Simulation of Depillaring Panel

5.1 General

FLAC^{3D} was used to implement the proposed explicit caving simulation approach. It is a tool for comprehensively modelling the structure while considering different geo-mining complexities. The overlying strata consist of different layers and are likely to separate due to weak interfaces during depillaring operations. The primary basis for selecting FLAC^{3D} is the capability to incorporate the appropriate failure criteria, interface, and controlling FLAC parameters through the FISH command. To implement the proposed explicit caving simulation approach, a case study of the bord and pillar depillaring panel is considered.

Steps for FLAC Modelling

Step 1- Define Objectives: Set goals for the analysis, such as stress redistribution or pillar behaviour.

Step 2- Create Geometry: Design the model layout with pillars, roof, floor, and goaf.

Step 3- Mesh the Model: Use fine grids in critical zones and coarse grids elsewhere for efficiency.

Step 4- Assign Properties: Input material parameters and interface properties.

Step 5- Set Boundaries: Apply displacement constraints and in-situ stress gradients.

Step 6- Simulate Mining: Sequentially remove pillars to mimic excavation.

Step 7- Model Time Effects: Incorporate time-dependent behaviour.

Step 8- Run and Verify: Execute the model and check for stability and accuracy.

Step 9- Analyse Results: Evaluate stress, deformation, and failure zones.

Step 10- Document Findings: Summarize inputs, processes, and results for clarity and reproducibility.

5.2 Case Study

A bord and pillar depillaring panel has been chosen to implement the proposed explicit caving simulation scheme. The study panel is located in the Peddapally district of Telangana state. The seam was developed using the bord and pillar system of mining with conventional drilling and blasting operations and depillaring was started after 20 years of the development. The developed seam was divided into a number of blocks, and the present block was considered for mechanised depillaring. The block consists of three proposed panels. During the study period, panel A had already been extracted, panel B was undergoing depillaring, and panel C was the developed panel. The panels are divided into sub-panels: the dip side with larger pillars and the rise side with smaller pillars.

5.2.1 Geo-Mining details

The layout of the study mine is shown in Fig. 5.1. The area had already been developed using conventional (drilling and blasting) methods. A continuous miner (CM) was proposed for depillaring operations after 20 years. Panel B consists of 85 pillars, and panel C consists of 78 pillars, excluding barrier pillars. Fig. 2 shows the nature of the overlying strata above the coal seam. The geo-mining information of a panel is given in Table 5.1. The seam has a gradient of 1 in 9, with a seam thickness of 5 m to 6 m. The depth of the panel varies from 172 m to 235 m. The size of the pillars in the panels varies from 35.5 m X 35.0 m to 35.5 m X 29.7 m from centre to centre. The dimensions of the galleries are 3.0 m x 4.8 m. To facilitate the CM operation, existing galleries have been widened

and heightened. The size of the galleries became 4.5 m x 5.5 m. The nature of the roof strata overlying the panel is depicted in a borehole section, as shown in Fig. 5.2. The average thickness of immediate strata is 5.0 m medium to coarse-grained sandstone, followed by 20 m fine-grained sandstone, 5.0 m thick medium to coarse-grained sandstone, and a thick 100.0 m and 30.0 m fine-grained sandstone. A clay bed was also observed in the borehole section.

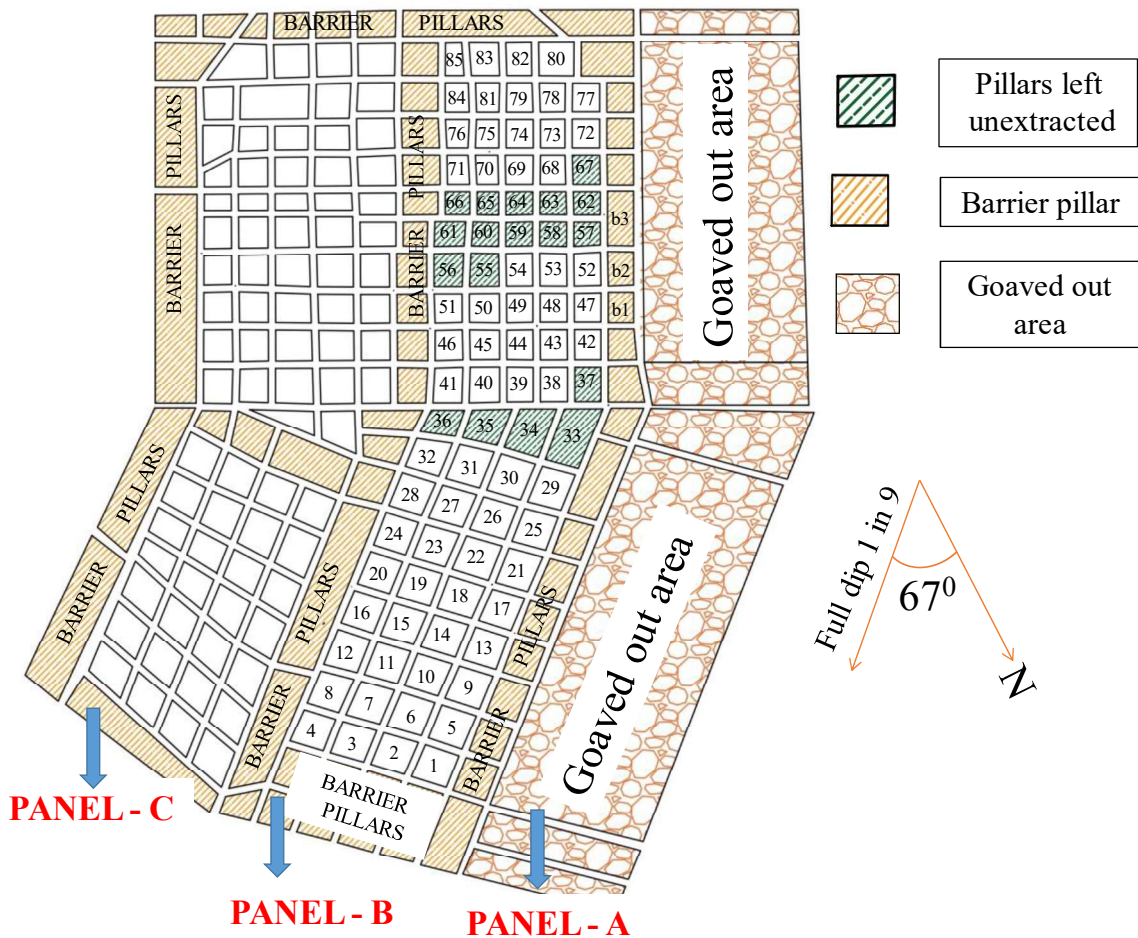


Figure 5.1: Mine layout with panels A, B and C

Table 5.1: Geo-mining details of the Mine

S.No	Parameters	Details
1	Dip direction of the coal seam	N 67 ⁰ E
2	A gradient of the coal seam	1 in 9
3	Working Depth	172.0 m to 235.0 m
4	Thickness of the seam	4 m to 6 m
5	The average width of the pillar (centre to centre) Dip side	35.0 m X 35.0 m
6	The average width of the pillar (centre to centre) Rise side	28.0 m X 28.0 m
7	width of gallery	6.0 m

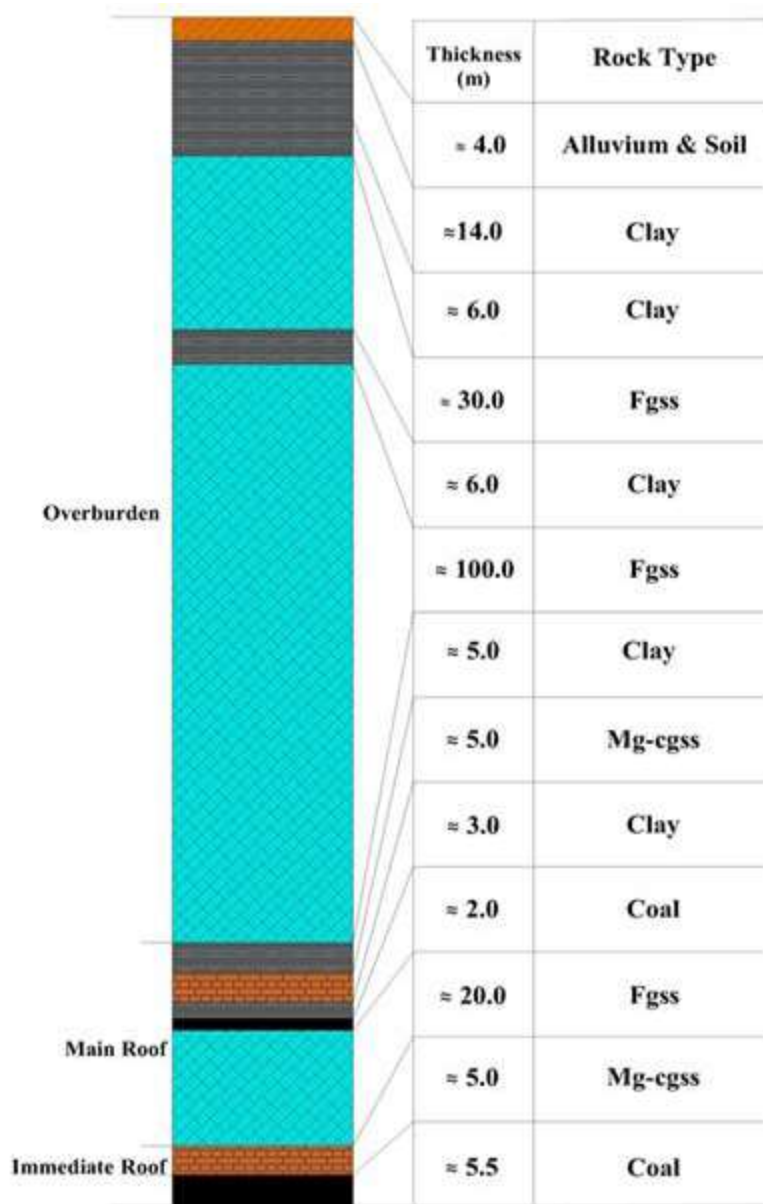


Figure 5.2: Generalised stratigraphy column

5.2.2 Method of working

Development and depillaring are the two main stages of underground bord and pillar mining. The depillaring has been proposed using the split and fender method. A straight line of extraction is adopted during depillaring operations. The sequence of the pillar extraction is shown in Fig. 5.1. During the slicing operation, a slice of coal from the floor has also been extracted. The extraction height has been considered a maximum of 5.5 m or up to the seam thickness, whichever is less.

5.2.3 Field observations

Various strata monitoring instruments like Dual Tell-Tale (DHTT), Vibrating Wire Stress Cells (VW), Rotary Tell-Tale (RTT), and Auto Warning Tell-Tale (AWTT) are used to monitor roof conditions. During depillaring operations, panel B encountered numerous strata issues, such as side spalling of pillars and irregular roof caving. Strata issues were noted on the dip side after extracting 32 pillars, including slight floor heaving towards the barrier. As a result, five pillars were left due to the large caving area on the dip side of the panel. On the rise side, side spalling was observed during the extraction of pillar number 49 in panel B and continued during the extraction and slicing of pillars 53 and 54, affecting both barrier and goaf edge working pillars. Thus, 13 pillars from pillars 55 to 67 (i.e., two rows of pillars) were left against the goaf. Based on the experience of strata issues in panel B, panel C was designed scientifically using numerical simulation techniques. Strata monitoring showed no issues, and the modified design was successfully implemented in the field. The first major fall occurred at a goaf area of 13,008 m² in panel B and 17,021 m² in panel C. Subsidence measurements after extracting panels A and B were 1.2 m and 1.16, respectively.

5.3 Numerical model Preparation

It is generally understood that the effect of the goaved-out panel will impact the adjacent panel. Therefore, a large model was created comprising three panels, A, B, and C. The discretisation of the model was done using eight-node elements (as shown in Fig. 5.3a). Based on the borehole section, the strata were modelled in different beds separated by the interfaces. The geometry of the model includes a floor, coal seam, and roof with different beds. The model includes a floor up to 30 m, which is considered an elastic material, while the coal and roof are elastoplastic materials. It is to be noted that strata failure has occurred within this zone (Peng 2008). The remaining model, i.e. from caving height to the surface, has been discretized coarsely with gradual increments, as shown in Figure 5.3. It is to be noted that all the beds are connected/separated by the interface element. Thus, for better accuracy, the ratio of the mesh size of the elements of both sides of the interface element shall be a maximum of 1.5 as suggested in the software manual (2015). Figure 5.3a shows the three-dimensional discretised view of the panel, and Figure 5.3b shows the sectional view of the model along the dip and rise sides.

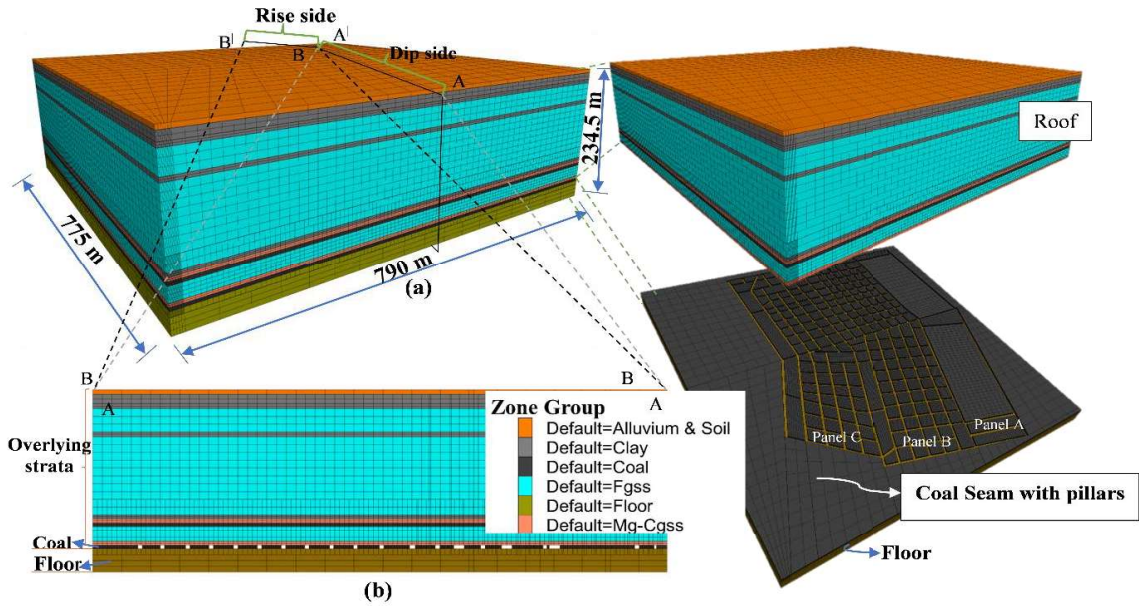


Figure 5.3: (a) Three-dimensional discretised view of the panel. (b) A sectional view of the model along A-A' in the dip side and along B-B' in the rise sides

5.3.1 Material Properties

Proper assigning of material properties to the model is necessary to get reasonable results. Various researchers (Murali Mohan et al. 2001; Kumar et al. 2017; Chawla and Jaiswal 2022) in the literature considered coal as Mohr-Coulomb material. Some researchers (Medhurst and Brown 1998; Jaiswal and Shrivastva 2009) considered coal as a Hoek-Brown material. In this study, Hoek-Brown failure criteria are considered for the coal seam, and the strength properties (m , s , and a) were taken from the literature suggested by Jaiswal (Jaiswal and Shrivastva 2009) for Indian cases. The strength properties considered for the coal seam in this model are $m = 1.47$, $s = 0.012$, and $a = 0.5$. Mohr-Coulomb failure criteria were considered for soft layers (clay) in the roof, and for the remaining layers, Hoek-Brown failure criteria were considered. Non-linear Sheorey's failure criterion (Sheorey 1997b) was used to deduce the rock mass properties. However, FLAC^{3D} cannot use Sheorey's failure criterion, so the Hoek-Brown failure criterion was chosen for simulating the model. The rock mass properties of strata (as shown in Fig.5.4) deduced from Sheorey's failure criterion are obtained using the following equations.

$$\sigma_1 = \sigma_{cm} \left(1 + \frac{\sigma_3}{\sigma_{tm}} \right)^{b_m} \text{-----} (5.1)$$

Where,

$$\sigma_{cm} = \sigma_{ci} \exp \left(\frac{RMR-100}{20} \right) \text{-----} (5.2)$$

$$\sigma_{tm} = \sigma_{ti} \exp \left(\frac{RMR-100}{27} \right) \text{-----} (5.3)$$

$$b_m = b^{RMR/100} \text{-----} (5.4)$$

Where σ_l is the tri-axial strength of the rock mass (MPa), σ_3 is the confining stress of the rock- mass (MPa), σ_{cm} is the compressive strength of the rock-mass (MPa), σ_{tm} is the tensile strength of the rock-mass (MPa), σ_{ci} is the compressive strength of the intact rock (MPa), σ_{ti} is the tensile strength of the intact rock (MPa) and RMR is the rock-mass rating (RMR) proposed by Bieniawski (Bieniawski 1976) in year 1976. In the above equations, the subscript m stands for the rock mass. Here, $\sigma_{ti} = \sigma_{ci} / 15$ and $b = 0.5$ has been considered the most representative values seen from many test data published earlier (Sheorey 1997a). The average RMR of the strata is considered 45. The non-linear Hoek-Brown failure criterion is expressed as follows.

$$\sigma_1 = \sigma_3 + \sigma_{ci} \left(m_b + \frac{\sigma_3}{\sigma_{ci}} + s \right)^a \text{-----} (5.5)$$

Where " σ_{ci} and σ_{ti} represent the tri-axial strength and confining stress of intact rock, m , s and a are the strength parameters of Hoek-Brown failure criterion". As suggested by Gadepaka (Gadepaka and Jaiswal 2023), the Hoek–Brown strength parameters for coal and overlying strata were deduced. Overlying strata are broadly classified into fine-grained sandstone and medium-grain to coarse-grained sandstone. A typical fine-grained sandstone graph is shown in Fig. 5.4. The rock strata properties of the model are shown in Table 5.2.

Strength parameters have been deduced by the trial and error method so that it must resemble the Sheorey failure criterion for a particular rock type. Fig. 5.4 shows the resemblance of Hoek–Brown and Sheorey’s failure criterion for a typical fine-grained sandstone. The Hoek- Brown criterion’s strength parameters, i.e. m , s and a , have been deduced as 1.4, 0.03 and 0.6, respectively. Similarly, this exercise has been carried out for other rock layers also. The computed results in terms of Hoek-Brown parameters, along with other physico-mechanical properties, have been shown in Table 5.2.

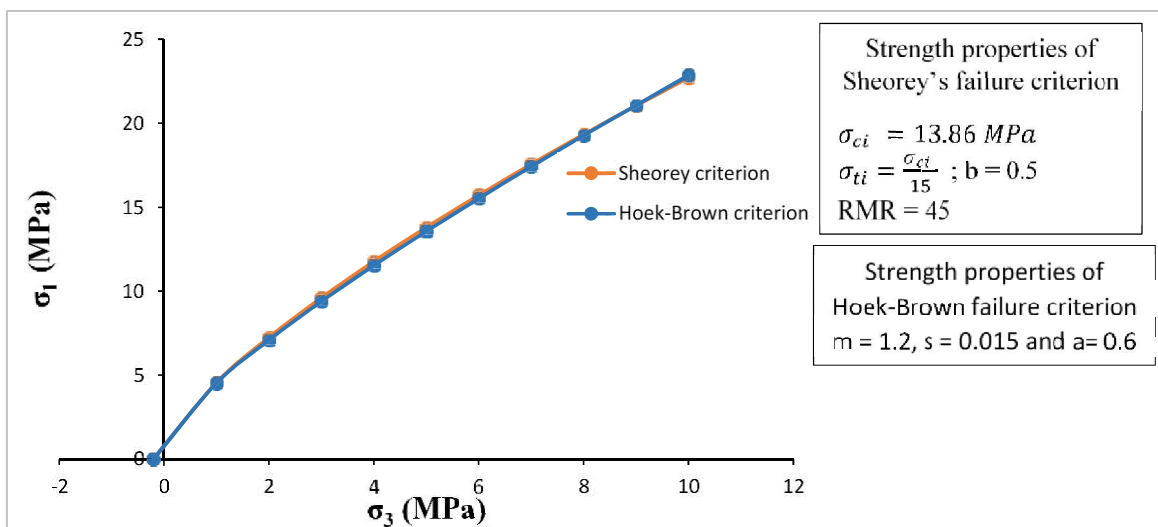


Figure 5.4: Approximation of Hoek–Brown with Sheorey’s failure criterion for a typical fine-grained sandstone

Table 5.2 Rock strata properties used in the numerical model

Rock bed	Density (kg/m ³)	Young’s modulus (GPa)	UCS (MPa)	Tensile strength (MPa)	Cohesion (MPa)	Friction angle (°)	Hoek-Brown strength parameters		
							m	s	a
Coal	1300	2	46.8	0.6	-	-	1.47	0.012	0.5
Clay	1600	3×10^{-3}	0.04	0.08	0.02	25	-	-	-
Medium to coarse-grained sandstone	2090	2.36	7.53	0.2	-	-	1.07	0.01	0.5
Fine-grained sandstone	2100	3.57	13.86	0.4	-	-	1.2	0.015	0.6

5.3.2 Interface Properties

Interface elements have been introduced between different layers characterised by coulomb sliding and/or tensile separation. These interface elements are used as parting planes in between layers. "A linear elastic-perfectly plastic coulomb shear strength criterion defines the constitutive model of the interface". The roof layers are likely to separate due to the introduction of interface elements. The Coulomb shear-strength criterion constrains the shear force through an equation.

$$F_{smax} = cA + \tan\phi (F_n + pA) \text{-----} (5.5)$$

Where " c is the cohesion along the interface (MPa), ϕ is the friction angle of the interface surface, and p is pore pressure (interpolated from the target face)". Pore pressure is not considered in this study. Input parameters of interface elements are properties of friction, cohesion, dilation, normal and shear stiffness. The stiffness values of the interface elements (Normal and Shear stiffness) were calculated from equation 5.6, as mentioned in the software manual (2015), which is verified by Wu et al.(Wu et al. 2011). A good thumb rule is to assign the normal stiffness (K_n) and shear stiffness (K_s) to be set ten times the equivalent stiffness of the stiffest neighbouring zone. The apparent stiffness (expressed in stress-per-distance units) of a zone in the normal direction is expressed in equation 5.6.

$$K_n = K_s = 10 \max \left[\frac{(3K+4G)}{\Delta Z_{min}} \right] \text{-----} (5.6)$$

Where K and G are bulk and shear moduli, respectively, and Z_{min} is the smallest dimension of an adjoining zone in the normal direction. The cohesion and tensile strength of interface elements were considered zero for all locations, and the friction angle was about 25^0 at various locations. Table 5.3 shows the interface element's properties at different overlying strata locations.

Table 5.3: Interface properties used in the numerical modelling at various locations

Location (from the coal seam in the upward direction)	Normal stiffness (Pa/m)	Shear stiffness (Pa/m)
At 9.5 m, 29.5 m, 39.5 m and 44.5 m	1.71×10^{10}	1.71×10^{10}
At 34.5 m	1.13×10^{10}	1.13×10^{10}
At 144.5 m and 150.5 m	1.43×10^{10}	1.43×10^{10}
At 180.5 m	1.2×10^7	1.2×10^7
At 186.5 m	2.0×10^{10}	2.0×10^{10}

5.3.3 In-situ stress and Boundary conditions

In-situ stresses (vertical and horizontal) are the stresses present in the ground prior to any excavation. Assigning the appropriate in-situ stress in a model is of utmost important. Vertical stress (σ_v) can be estimated using equation 5.7. Horizontal stress (σ_h) (major and minor) can be estimated using field experiments (such as the hydro-fracturing method). In the present study horizontal stresses have not been determined using a field experiment. Therefore, it has been estimated using the empirical approach proposed by Sheorey (1994) (Sheorey 1994) as expressed in equation 5.8.

$$\sigma_v = \rho g H \text{-----} (5.7)$$

$$\sigma_h = \frac{\nu}{1-\nu} \sigma_v + \frac{\beta E G}{1-\nu} (H + 1000) \text{-----} (5.8)$$

Where ρ is the material's density, g is the acceleration due to gravity, H is cover depth in m, σ_v and σ_h are vertical and horizontal in-situ state of stresses in MPa, E is Young's modulus in GPa , and β is the coefficient of thermal expansion in ($^{\circ}C$), G is the geothermal gradient ($^{\circ}C/m$). The value of β has been considered $8 \times 10^{-6} /^{\circ}C$ and $30 \times 10^{-6} /^{\circ}C$ respectively for sandstone and coal. The value of G has been used $0.03^{\circ}C/m$ in this model for all the layers. All the beds in the roof have different vertical and horizontal in-

situ stress based on the depth and density of the material. With the availability of software package (2015) a gradient was used to reproduce the effects of stress with increasing depth caused by gravity.

$$S = S^{(0)} + (g_x \cdot H) + (g_y \cdot H) + (g_z \cdot H) \text{-----} (5.9)$$

Where $S^{(0)}$ stress value at the origin ($x = 0, y = 0, z = 0$), g_x , g_y and g_z are the gradient value in x, y and z directions.

The roller boundary condition has been assigned to the vertical walls of the model in the lateral dimensions (i.e., X and Y) to restrict the movement in lateral X and Y directions. The bottom of the model has been assigned with fixed boundary condition in the Z direction. Whereas, top of the model has been kept unrestricted so that grids can be moved in downward direction during the depillaring operation.

5.3.4 Scheme of simulation

A standard procedure has been used to simulate the caving behaviour of strata with a progressive advancement of the face in a depillaring panel. After the development of the model required material properties, in-situ stress conditions and boundary conditions have been assigned. A FISH program has been written to restrict the uncontrolled deformation of the immediate roof and attach it to the floor. The straight line of extraction of coal pillars has been considered. Thus, a program has been written to remove the coal pillars in each stage of excavation. The model has been solved till the structures get nearly equilibrium condition (i.e. unbalanced force equal to $1e^{-5}$). The results have been saved after the completion of each depillaring stage. A FISH module has been programmed to calculate the average vertical stress on pillars during the progressive advancement of the face.

5.4 Concluding remarks

A case of bord and pillar mine with three panels (panels A, B and C) has been chosen. The panel comprises two sub-panels: the dip side with larger pillars and the rise side with smaller ones. A three-dimensional model of the depillaring panels has been created in FLAC^{3D}. Interface elements are used between the layers to enable layer separation if it occurs during the mining operation. The rock-mass properties of the overlying strata were deduced by considering Sheorey's failure criterion. Hoek-Brown strength parameters of overlying strata have been deduced by the trial and error method so that it must resemble the Sheorey failure criterion.



